Optical and Raman investigation of Yb pnictide compounds

L. Degiorgi, S. Teraoka,* G. Compagnini,† and P. Wachter
Laboratorium für Festkörperphysik, Eidgenössische Technische Hochschule Zürich, CH-8093 Zürich, Switzerland
(Received 10 September 1992)

We report on our thorough optical investigations of the Yb pnictide compounds, performed over a large photon-energy spectral range. From Kramers-Kronig analysis we obtain the complete excitation spectrum in terms of the optical dielectric functions. Applying a phenomenological harmonic-oscillator model we extract the unscreened plasma frequency and the resonance frequency of the transverse-optical-phonon mode. Our experimental findings suggest furthermore a d-$4f$ electronic transition at about 0.2 eV, in agreement with high-energy electron-spectroscopy results. We also report on our Raman-effect measurements. Moreover, we compare our results with the reference material ScN and we discuss the influence of nonstoichiometry in the Yb pnictides.

I. INTRODUCTION

The physical properties of the rare-earth pnictides continuously deserve a lot of interest both experimentally and theoretically. Above all, their electronic structure, where localized ($4f$) and extended valence states coexist in the same energy range, makes these systems particularly attractive and intriguing.

Prototypes of this class of compounds are the Yb pnictides, which like all the rare-earth pnictides crystallize in the face-centered cubic (fcc) rocksalt structure. Since there exists an indirect overlap of the pnictide p bands [maximum at the Γ point of the Brillouin zone (BZ)] and the rare-earth d bands (minimum at the X point of BZ), these materials are semimetals. They are also considered as "mirror-systems" to the much studied Ce compounds, inasmuch as their $4f$ shell contains zero or one hole (i.e., a many-body $4f^{13}$ or $4f^{14}$ state). As such, the degenerate Anderson impurity model was applied to the study of their high-energy electron spectra [i.e., photoemission (XPS), bremsstrahlung (BIS), and core-level spectroscopy] in the theoretical framework originally given by Gunnarsson and Schoenhammer[1] for the Ce compounds by simply inverting the energy scale.[2] The Yb pnictides also undergo a phase transition below 1 K, suggestive of a magnetically ordered ground state. In fact, Mössbauer spectroscopy proved the magnetic origin of the phase transition,[3] and neutron diffraction experiments showed the ordering to be antiferromagnetic of type III in stoichiometric YbAs and YbN, and of type II in nonstoichiometric YbP.[4–6]

Furthermore, the occurrence of a broad hump in the specific heat of all Yb pnictides around 5 K, with no apparent relation to the Schottky anomaly expected from the crystal field splitting, has led to the conjecture that the quasiparticles in these compounds are heavy fermions.[7] Recently, it was, however, shown theoretically that the above feature is a natural consequence of the interplay between crystal field and Kondo effect for an isolated magnetic impurity, and the coherent or Bloch-type nature of the quasiparticle states need not be invoked.[8] By performing several measurements on well-characterized single crystals of YbN, we also arrived at similar conclusions.[9] In fact, we clearly stated that YbN is not a heavy fermion but rather a weakly intermediate valent system with Kondo characteristics. The latter feature is further enhanced in nonstoichiometric samples.[9]

The aim of the present work is to systematically review our thorough optical investigations (i.e., reflectivity measurements and Raman spectroscopy) on the YbN, YbP, and YbAs series. The employed experimental techniques, and the experimental results are presented in Sec. II, while the discussion of our findings is presented in Sec. III. Finally, in Sec. IV we summarize our main conclusions. Some of the results were discussed elsewhere.[9]

II. EXPERIMENTS AND RESULTS

The specimens used in our investigations were prepared following the procedure already described in detail in earlier publications.[9,10] Briefly, the main point is that the handling of the metal and the compound has been performed in argon glove boxes gettered by hot cerium turnings having a residual oxygen concentration of less than 3 ppm. This ensures crystal growth conditions which are free from oxygen contamination. The chemical analysis and x-ray crystallographic investigation show that the materials are stoichiometric ($\pm 0.5\%$) and only the rocksalt structure has been detected. The large single crystals used in this work are between 3 mm and 5 mm edge length and have a lattice constant of 4.781 Å (4.784 Å), 5.5375 Å, and 5.6975 Å for YbN ($YbN_{0.96}$), YbP, and YbAs, respectively.

The Yb pnictides compounds were also characterized by the measurement of the electrical resistivity with a conventional four-probe method and of the Hall effect employing the van der Pauw technique. The resistivity for the stoichiometric samples is presented in Fig. 1. At room temperature ρ_{dc} has been found to be 10.5×10^{-5} (Ωcm) for YbN, 7.5×10^{-5} (Ωcm) for YbP, and 5.7×10^{-5} (Ωcm) for YbAs, with a metallic temperature coefficient. The negative Hall effect leads to a carrier concentration of $N_e=4.8\times10^{20}$ cm^{-3} for the stoichiometric YbN (Ref. 9) and $N_e=1.2\times10^{21}$ cm^{-3} for YbP, using an effective one-band model.

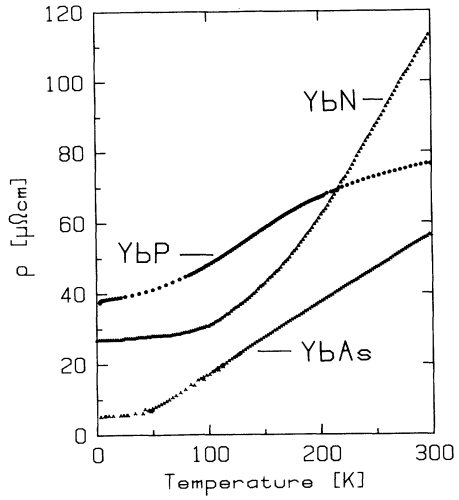

FIG. 1. Resistivity vs temperature for YbN, YbP, and YbAs.

The optical reflectivity of YbN, YbP, and YbAs has been measured in a photon energy range from 12 eV down to 1 meV at room temperature [and in the far-infrared (FIR) spectral range also at 6 K] using four spectrometers. In the FIR part of the spectrum we have employed a Bruker Fourier transform interferometer with a Hg arc light source, and a triglycene detector down to 50 cm^{-1} and a liquid helium-cooled germanium bolometer detector from 100 to 10 cm^{-1}. The data from different spectrometers and/or source-detector combinations showed a mismatch of maximum 3%.

Figures 2(a)–2(c) show the whole reflectivity spectra [$R(\omega)$] at 300 K of YbN, YbP, and YbAs, respectively. The low-temperature data are practically unchanged. Only in nonstoichiometric YbN compounds (i.e., $YbN_{0.96}$) a remarkable temperature dependence of $R(\omega)$ was detected in the FIR [see inset of Fig. 2(a)].[9] The arrow in Fig. 2(b) marks the presence of a shoulder in the YbP spectrum, which appears in the midinfrared at ~0.2 eV (2000 cm^{-1}). The latter feature is well resolved in YbN also at 0.2 eV while it is not clearly detected in YbAs.

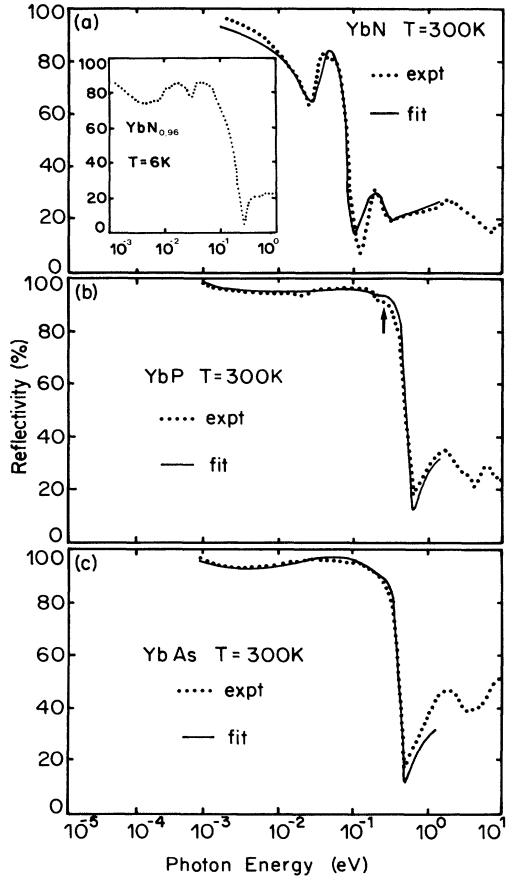

FIG. 2. Reflectivity spectra $R(\omega)$ at 300 K of YbN (a), YbP (b), and YbAs (c). The arrow in (b) indicates the shoulder at 0.2 eV superimposed to the plasma edge. The inset in (a) shows the $R(\omega)$ of nonstoichiometric YbN (i.e., $YbN_{0.96}$) at 6 K. The solid line is the phenomenological fit (see text).

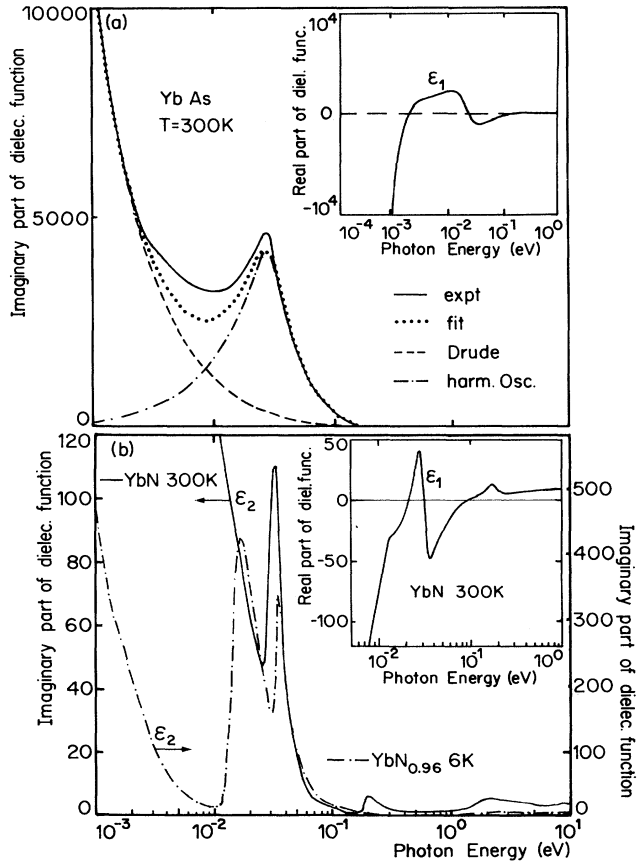

FIG. 3. (a) Imaginary and real (inset) parts of the dielectric function of YbAs obtained by KK transformation of $R(\omega)$ in Fig. 1(c). The phenomenological fit with its various components is also presented (see text and Table I for the parameters). (b) Dielectric function of YbN at 300 K and of $YbN_{0.96}$ at 6 K, as evaluated by KK transformation of $R(\omega)$ in Fig. 1(a).

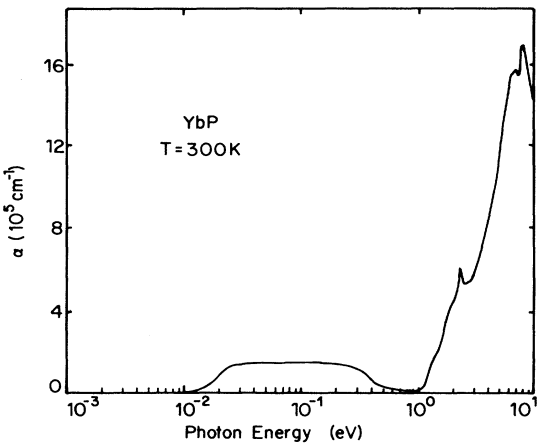

FIG. 4. The absorption coefficient α of YbP at 300 K.

These $R(\omega)$ spectra extending over more than four decades of photon energy are subsequently used for Kramers-Kronig (KK) transformation. The frequency range of the measured reflectivity spectrum has been extrapolated toward zero frequency by means of the Hagen-Rubens relation using the σ_{dc} values and for energies larger than 12 eV the reflectivity has been assumed to drop off as ω^{-2} and above 18 eV as ω^{-4}. From this analysis one gets the complete set of optical functions like the dielectric function $\varepsilon(\omega)$ and the optical conductivity $\sigma(\omega)$. The imaginary (ε_2) and real (ε_1) part of the dielectric functions of YbAs are presented in Fig. 3(a), while Fig. 3(b) presents the complex dielectric function components of YbN at 300 K and of the nonstoichiometric $YbN_{0.96}$ at 6 K.[9] YbP has dielectric functions similar to YbAs. Nevertheless, we present in Fig. 4 the absorption coefficient $\alpha=2\omega k/c$ of YbP, where k is the absorption constant.

The Raman spectra were measured at 300 K using a 5145-Å-laser excitation. Figure 5 shows the Raman spectra of YbN, YbP, and YbAs at 300 K. For the purpose of the following discussion we display in Fig. 5 also the Raman results of ScN.[9]

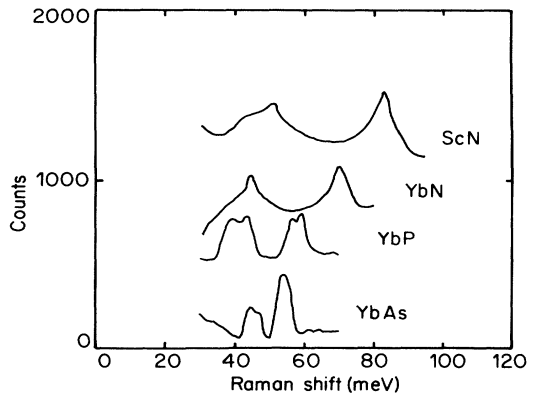

FIG. 5. Raman shift of YbAs, YbP, and YbN compared with ScN at 300 K.

III. DISCUSSION

First of all, we note that the dc transport measurement of Fig. 1 and the $R(\omega)$ spectra (which tend to 100% as $\omega\rightarrow 0$) of Fig. 2 are suggestive of a metallic behavior. Moreover, we remark the hump at about 200 and 150 K (although weak) in the $\rho(T)$ curve (Fig. 1) of YbP and YbAs, respectively. This peculiar behavior of $\rho(T)$ has to be contrasted with the relative normal $\rho(T)$ of YbN, which shows a saturation to a residual resistivity of about 3×10^{-5} Ωcm at already 100 K. Although an impurity effect cannot be completely ruled out, the origin of the hump is probably related to the crystal field splitting of the $4f$ states. Indeed, neutron scattering investigations suggest crystal field splitting excitations above 300 K for YbN and around 200 K for YbP and YbAs.[4–6] Our anomalies in $\rho(T)$ at 200 and 150 K for YbP and YbAs, and their absence below 300 K in YbN would be then consistent with the trend of the neutron scattering results. Anyway, the metallic behavior is expected since, as has already been mentioned in the Introduction, by symmetry considerations the rare-earth pnictides are self-compensated semimetals with an indirect overlap of p and d bands. The metallic characteristics arrived at by both transport, and thermo- and electrodynamic investigations[7,9] is in striking contrast with recent results, which suggest a semiconducting behavior in LnP (where Ln=La, Nd, Sm, and Y).[11] This is a well-known controversy, which reminds us of a 20-yr-old debate.[9] Only in the last decade with perfect and stable stoichiometric crystals a general consensus on the semimetallic properties of the Yb pnictides has been achieved. Thus, the reason for such a discrepancy has to be ascribed to nonstoichiometric crystals most probably also with a high level of oxidation.

We develop our discussion as follows: first with the aid of a phenomenological fit based on the classical dispersion theory we will discuss the main ingredients associated with the electrodynamic response of the Yb pnictides. Second, we will discuss the phonon spectrum, while the plasmon and the interband transitions will be treated in a third section. Finally, our discussion will give some attention to the temperature dependence of the electrodynamic properties in the Yb pnictides with particular emphasis on nonstoichiometric YbN.

A. Phenomenological fit of the reflectivity

We describe the optical response due to the free charge carriers with the Drude model. Superimposed on this metallic contribution we recognize a well-defined hump which clearly appears in our spectrum of YbN at approximately 30 meV,[9] while it has a somehow broad character in YbP and YbAs. Above the so-called screened plasma edge [i.e., at ~0.1 eV in YbN and at ~0.5 eV in YbP and YbAs, which is the onset of the metallic behavior in $R(\omega)$], various excitations associated to interband electronic transitions (see discussion below) characterize the electrodynamic response at these high frequencies. In

particular, we want to emphasize the excitation at 0.2 eV in the stoichiometric YbN which has a single Lorentzian line shape.[9] The latter feature is present in the form of a shoulder in YbP and nonstoichiometric YbN (see arrow in Fig. 2) but it is hardly detected in YbAs.

In order to quantitatively describe our $R(\omega)$ spectra, we apply a phenomenological approach, based on a harmonic oscillator (h.o.) model. We model the dielectric function as follows:

$$\varepsilon(\omega)=\varepsilon_1+i\varepsilon_2 = \frac{\omega_p^2}{-\omega^2+i\gamma\omega}+\sum_{i=1}^{3}\frac{\omega_{pi}^2}{\omega_i^2-\omega^2+i\gamma_i\omega}+\varepsilon_\infty . \quad (1)$$

The first term describes the response due to a simple Drude law and is defined by the unscreened plasma frequency ω_p and the damping γ. The three harmonic oscillators are characterized by the resonance frequencies ω_i, the mode strengths ω_{pi}, and the dampings γ_i. Finally, the high-frequency (i.e., $\omega\rightarrow\infty$) contribution to $\varepsilon(\omega)$ is incorporated by ε_∞. We first apply this phenomenological h.o. approach to stoichiometric YbN. The h.o. are ascribed to the FIR excitation at about 30 meV, to the interband transition at 0.2 eV, and to the broad high-frequency excitation centered at about 2 eV. Subsequently, we fitted the $R(\omega)$ spectra of YbP and YbAs, where the electronic transitions at 0.2 and at 2 eV were described by the same set of parameters previously obtained for YbN. The full set of parameters used for our fits is summarized in Table I. The continuous line in Fig. 2 shows the fit to $R(\omega)$, and the contributions in the FIR of the Drude and h.o. at about 30 meV are also shown for $\varepsilon_2(\omega)$ of YbAs in Fig. 3(a).

B. Phonon spectrum

The excitation in the FIR at approximately 30 meV in YbN (i.e., ω_1 in our fit) is ascribed to the transverse optical (TO) phonon of the rocksalt structure at the Γ point of the BZ, which can be excited by light. We observe also that the phonon frequencies are appreciably softened compared with ScN (i.e., at approximately 50 meV).[9] This is reasonable because of the larger reduced mass of the Yb pnictides compared with ScN. From our fit (Table I) we also observe a small softening of the TO phonon frequency in the Yb pnictides which is again the consequence of the increasing reduced mass when spanning from N to As in this series.

TABLE I. Parameters of the harmonic oscillator phenomenological fit: plasma frequency ω_p and damping γ of the Drude model, resonance frequencies ω_i, dampings γ_i, and mode strengths ω_{pi} of the harmonic oscillators, and high-frequency dielectric constant ε_∞.

Parameter (eV)	YbN	YbP	YbAs
ω_p	0.2	0.74	0.74
γ_p	0.02	0.05	0.124
ω_1	0.034	0.026	0.022
γ_1	0.01	0.038	0.0124
ω_{p1}	0.19	0.19	1.3
ω_2	0.2	0.2	0.2
γ_2	0.1	0.1	0.1
ω_{p2}	0.35	0.35	0.35
ω_3	2.0	2.0	2.0
γ_3	1.5	1.5	1.5
ω_{p3}	4.9	4.9	4.9
ε_∞	1.0	7.0	7.0

From recent investigations about the elastic properties of the whole Yb pnictide series it is possible to extract the spring force constant (f) characterizing the nearest-neighbor ionic interaction of these NaCl structure materials.[12] Within a simple 1-dimensional approach based on the harmonic approximation one can calculate the frequency of the TO phonon mode with the formula $\omega_{TO}=(2f/m_r)^{1/2}$, where m_r is the reduced mass. It turns out that f is almost constant for all compounds[12] and the calculated ω_{TO} are 50, 35, and 25 meV for YbN, YbP, and YbAs, respectively, in fair agreement with the measured and fitted (ω_1 in Table I) frequencies.

Additional information regarding the phonons can be obtained from Fig. 5 where we show the Raman measurements of the Yb pnictides and of ScN. In Yb pnictide compounds the rocksalt crystal structure prohibits the first-order Raman effect. However, from the defect-induced first-order Raman scattering one can obtain the perturbed projected phonon density of states, with sharp features associated with the Van Hove singularities. In Fig. 5 are shown two Raman peaks for each sample. Since the largest density of states is observed at the L point of the BZ, i.e., at the zone edge, optical phonons detected with Raman spectra cannot be compared directly with the TO phonons found with FIR reflectivity investigations and which can be related to the Γ point only.

The high-energy peak strongly shifts to lower energy going from YbN to YbAs, while the lower one appears almost at the same frequency for all Yb pnictides (besides a small shift upward in YbAs). It is worthwhile to remark that the lower energy Raman mode splits clearly in a double structure in YbP and has a pronounced shoulder to the lower energy side in YbN and YbAs. In the high-energy mode, a double-peak structure appears only in YbP. The presented Raman spectra bear an interesting parallelism with the Raman investigations on other compounds with NaCl structure; namely TiN,[13] TiC,[14] NaI,[15] and of course ScN.[9,16]

The Raman modes of the Yb pnictides in Fig. 5 are related to the optical branches of the dispersion relation, and more precisely to those points of the BZ with the highest phonon density of states. Such a high density of states is achieved at the L (as stated above), and X points of BZ, and also at the maximum along the [110] direction of the reciprocal space.[14,15] It was also suggested that in extremely pure (i.e., stoichiometric) samples one can detect linear combinations of longitudinal and transverse acoustic (LA or TA) and/or optical modes (LO or TO).[13] In this respect, one can be tempted to assign the lowest Raman mode in the Yb pnictides with the 2LA or 2TA or LA+TA excitations. Although this might be particularly compelling in relation to the experimental observation that this mode appears at the same frequency for all

Yb pnictides, we judge this possibility quite unlikely.

It is important here to advise the reader that our spectra of the Yb pnictides *do not* show the (true) acoustic mode (TA or LA). In this regard, the comparison with the Raman spectra of ScN (Fig. 5) can be somehow misleading, since the two Raman structures (at about 50 and 80 meV) in this case are assigned indeed to the acoustic (lower one) and optical (higher one) branch, respectively. This is also supported by the comparison of the Raman mode between ScN and TiN or TiC.[16] Furthermore, the frequency of the acoustic mode of the Yb pnictides is calculated by the relation $(2f/M_{\mathrm{Yb}})^{1/2}$,[12] or by a simple mass scaling argument (i.e., assuming that the elastic constants do not change dramatically) of the acoustic mode in TiN, TiC, NaI, and ScN.[13–16] The expected frequency for the Yb pnictide acoustic mode is much too low (i.e., lower than 20 meV) in order to be detected. Moreover taking into account that the lattice constant might also be slightly different [i.e., the Yb pnictides are expected to be even softer (smaller f) than ScN], one realizes immediately that the so-evaluated acoustic mode frequency of about 20 meV is an upper limit. It is also worth noting that recent neutron scattering investigation on YbN clearly shows phonon peaks between 15 and 20 meV.[5] A detailed calculation of the dispersion relation of the Yb pnictides starting from the measured elastic properties is left for the future.[12]

C. Plasmon and interband transitions

The unscreened plasma frequency ω_p is higher in YbAs and YbP than in YbN. This may be explained by a reduced concentration of charge carriers and/or an enhanced optical mass in YbN. In this respect and as already performed for the nitride compound,[9] it is instructive to compare ω_p of the Yb pnictides with that of the reference compound ScN. The latter is isostructural with the rare-earth pnictides but does not contain $4f$ states. As such the electronic structure can be investigated theoretically with a reliable band-structure calculation,[17] which was found to be compatible with experimental findings.[16] The ratio of the corresponding squared plasma frequencies is proportional to the ratio of the charge-carrier concentration times the inverse ratio of the effective optical mass. Using for ScN $m_0 \approx 0.13 m_e$ and $\hbar\omega_p \approx 0.9$ eV,[16] and the carrier concentration obtained by Hall effect measurements, we have obtained $m_0 \approx 2.23 m_e$ and $m_0 \approx 0.4 m_e$ for YbN (Ref. 9) and YbP, respectively. Then, it is fair to assume that the optical mass for YbAs is the same as in YbP (i.e., $\sim 0.4 m_e$). This would imply a carrier concentration of the order of 10^{21} cm^{-3} for YbAs.

Let us turn now to the higher frequency part of the spectrum which we described in terms of the h.o. centered at 0.2 eV (ω_2) and at 2 eV (ω_3) and of ε_∞. The detailed electronic structure of YbN was already described and discussed elsewhere.[9] The electrodynamic response at frequencies from the visible up to the ultraviolet of YbAs and YbP is practically nondistinguishable from that of YbN. Similar optical fingerprints of the electronic excitations (i.e., mainly due to the typical p-d interband transitions) are in fact expected since the general features of the band structure are the same in the whole Yb pnictides series. In summary, we note that, besides the electronic transition at 0.2 eV discussed below, the next high-energy electronic transitions are found at nearly 0.4 and 0.8 eV in YbN. They were associated with direct optical transitions near the X point of the BZ, consulting the self-consistent band-structure calculation of ScN.[17] The dominant peak at 2 eV corresponds to the direct gap at the Γ point of BZ, which develops due to the mixing of the p valence band and the bare $4f^{13}$ state. This hybridization introduces a spectral repulsion, shifting furthermore the p band closer to the d band. The transitions at 6 and 7 eV correspond to the W point and at 12 eV to the L point of BZ.[9] Of course the latter proposals must await a quantitative confirmation from joint density of states and matrix element calculations.

We want to emphasize now the peculiarity of the transition at ~ 0.2 eV, which is clearly recognized in YbN [Fig. 2(a)]. A comparison with photoemission (XPS) and inverse-photoemission (BIS) spectra on YbP (Ref. 18) led to the conclusion that the optical transition at 0.2 eV involves f and d states.[9] Indeed, the photoemission spectra demonstrate that the minimum energy for the excitation of a $4f^{13}$ electron into the vacuum is approximately 6 eV below the Fermi level (E_F). At about 2 eV below E_F there is a hump which is due to p-valence electron emission. The p bands extended up to E_F. Above E_F the BIS measurement displays the unoccupied spherically symmetric $4f^{14}$ state at about 1 eV and at much higher energies the d bands, which commence right at E_F and overlap slightly with the p valence bands. The transition at 0.2 eV is then ascribed to an excitation from a d electron at E_F into the empty $4f^{14}$ state which we expect to be very close to, but above E_F.[9] This is also supported by the absence of the corresponding peak in the energy loss spectrum of ScN (see Fig. 7 in Ref. 9). In nonstoichiometric YbN,[9] and in YbP and YbAs as well, which have a larger $\omega_p (> 0.3$ eV) than the stoichiometric YbN, such a transition is almost completely screened by the plasma edge. However, YbP shows a weak shoulder superimposed to the plasma edge [see arrow in Fig. 2(b)], which, we believe, is another indication of this optical excitation. Furthermore, this intuition is confirmed by the broad feature in the absorption coefficient of YbP (Fig. 4) and also by the fact that only by including the h.o. at 0.2 eV we can reproduce within our phenomenological approach the shoulder found experimentally in YbP [Fig. 2(b)]. A weak shoulder can be recognized also in the $R(\omega)$ spectrum of the nonstoichiometric YbN [inset of Fig. 2(a)]. Although in YbAs a shoulder is hardly visible, we are convinced that this is a remarkable and intrinsic feature in the electrodynamic response of the Yb pnictides.

D. Temperature dependence and the nonstoichiometric problem

Finally, we would like to point out again the temperature independence of our $R(\omega)$ spectra for the stoichiometric Yb pnictides. This contrasts with the situation of the nonstoichiometric $YbN_{0.96}$ [see inset Fig. 2(a)], where a further absorption at approximately 17

meV and below the TO mode develops upon cooling toward 6 K [Fig. 3(b)]. We have suggested that the higher charge concentration due to the nonstoichiometry allows a partial occupation of the $4f^{14}$ state (which lies 0.2 eV above E_F in the stoichiometric YbN).[9] In fact, the salient and unexpected feature of YbN is the position of the empty $4f^{14}$ (or one-hole) state about 0.2 eV above the Fermi level as evidenced by BIS and optical spectroscopy (as discussed above). This $4f^{14}$ state hybridizes with the empty $5d$ band and results in a narrow hybridization gap. Since these levels are unoccupied in the stoichiometric compound, we do not expect much influence on physical properties. When the material becomes nonstoichiometric then we measure a larger carrier concentration so that the Fermi level enters somewhat the hybridized $4f^{14}$ state resulting in an f-d Kondo effect. Thus, the transition at 17 meV corresponds to the excitation across the so-called hybridization gap, or in other words to the transition between the two narrow bands formed in the density of states by the hybridized $4f^{14}$ state with the $5d$ bands (see Fig. 9 in Ref. 9). This new effect leads also to a slightly renormalized plasma frequency, and consequently to an enhanced effective optical mass (i.e., $m_0 \approx 6m_e$).[9]

IV. CONCLUSION

We have reported on our complete optical and also Raman effect investigation of the YbN, YbP, and YbAs series. The electrodynamic response is ascribed to the combined contribution of a Drude term and of transverse optical phonon and electronic interband excitations. This description is consistent with the semimetallic nature of these compounds and with their rocksalt structure, respectively. Of particular interest is then the interband transition in the midinfrared (at 0.2 eV), which has also its counterpart in the high-energy electron spectra and which reveals the position of the empty $4f^{14}$ state. Our investigation on chemically well characterized and stoichiometric compounds does not reveal any temperature dependence of the optical response. However, we pointed out the important consequences of nonstoichiometry in YbN on the temperature dependence of the electrodynamic response.[9]

Although the Yb pnictides (stoichiometric or nonstoichiometric) are moderate Kondo systems but not heavy fermions,[7] it is suggested that with application of hydrostatic pressure or by alloying with tetravalent metals the carrier concentration in the $4f^{14}$ state can probably be enhanced. The so-obtained higher occupancy of this $4f^{14}$ state may lead the Fermi level to coincide with the density of state maximum, resulting in large effective mass, an enhanced γ value of the specific heat, and possibly heavy fermion characteristics. These experiments are left for the future.

ACKNOWLEDGMENTS

The authors are grateful to M. Mendik for his preliminary measurements of the elastic properties of the Yb pnictides and for useful discussions, and also acknowledge the technical help of J. Müller, H. P. Staub, and P. Dekumbis. The single crystals of YbN and YbP have been grown by Professor E. Kaldis and those of YbAs by Dr. F. Hulliger to whom the authors are very grateful. One of us (L.D.) would like to acknowledge the financial support of the Swiss National Foundation for the Scientific Research.

*Present address: Tokyo Institute of Technology, Dept. of Physics, Tokyo 152, Japan.

†Present address: Universitá di Catania, Dip. di Fisica, IMETEM-C.N.R., I-95129 Catania, Italy.

[1] O. Gunnarsson and K. Schoenhammer, Phys. Rev. B **28**, 4315 (1983).

[2] R. Monnier, L. Degiorgi, and D. D. Koelling, Phys. Rev. Lett. **56**, 2744 (1986).

[3] P. Bonville, J. A. Hodges, F. Hulliger, P. Imbert, and H. R. Ott, J. Magn. Magn. Mat. **63-64**, 626 (1987).

[4] A. Doenni, P. Fischer, A. Furrer and F. Hulliger, Solid State Commun. **71**, 65 (1989).

[5] A. Doenni, P. Fischer, A. Furrer, W. Bacsa, and P. Wachter, Z. Phys. B **80**, 269 (1990).

[6] A. Doenni, A. Furrer, P. Fischer, F. Hulliger, P. Wachter, and H. R. Ott, J. Magn. Magn. Mat. **90-91**, 143 (1990).

[7] H. R. Ott, H. Rudigier, and F. Hulliger, Solid State Commun. **55**, 113 (1985).

[8] R. Monnier, L. Degiorgi, and B. Delley, Phys. Rev. B **41**, 573 (1990).

[9] L. Degiorgi, W. Bacsa, and P. Wachter, Phys. Rev. B **42**, 530 (1990).

[10] E. Kaldis, B. Steinmann, B. Fritzler, E. Jilek, and A. Wisard, in *The Rare Earths in Modern Science and Technology,* edited by J. McCarthy *et al.* (Plenum, New York, 1982), Vol. 3, p. 224.

[11] M. Jian and R. Yufang, Solid State Commun. **80**, 485 (1991).

[12] M. Mendik and P. Wachter, this issue, Phys. Rev. B **47**, 6110 (1993).

[13] W. Kress, P. Roedhammer, H. Bilz, W. D. Teuchert, and A. N. Christensen, Phys. Rev. B **17**, 111 (1978); W. Spengler, R. Kaiser, A. N. Christensen, and G. Müller-Vogt, *ibid.* **17**, 1095 (1978).

[14] A. Treindl, Ph.D. thesis, ETH-Zürich, 1981.

[15] P. Brüesch, in *Phonons: Theory and Experiments I,* edited by M. Cardona, P. Fulde, and H. J. Quessier (Springer-Verlag, Berlin 1982).

[16] R. Monnier, J. Rhyner, T. M. Rice, and D. D. Koelling, Phys. Rev. B **31**, 5554 (1985).

[17] G. Travaglini, F. Marabelli, R. Monnier, E. Kaldis, and P. Wachter, Phys. Rev. B **34**, 3876 (1986).

[18] E. Wuilloud, Ph.D. thesis, University of Neuchatel, 1986.